

Chapter 12

A Note on Imbricated Granite Boulders on NW Penang Island, Malaysia: Tsunami or Storm Origin?

Sharad Master

Abstract The Batu Feringgi area (N coast, Penang Island), with a high concentration of beach hotels, is critical to the tourist economy of Malaysia. Three large imbricated granite boulders were discovered on the NE end of the beach, at $5^{\circ}28'51.77''\text{N}$, $100^{\circ}15'72''\text{E}$. These boulders, dipping 45° – 70° seaward, are shaped as tabular parallelepipeds with rounded corners, with maximum masses of 1.1–2.4 t, based on a density of 2.71 g/cm^3 . The boulder shapes were dictated by the presence of joints in the coastal outcrops, which represent an uplifted and exhumed tropically-weathered granite-tor landscape.

In order to produce imbrication of several boulders, the mode of transport has to be rolling/overturning, rather than by sliding or saltation. The hydrodynamic equations for the initiation of boulder transport used in this study are the modified Nott equations, from Nandasena et al. (Marine Geology 281:70–84, 2011). Calculations were made using slopes of 2° and 5° .

The results of the calculations indicate that the minimum velocities required to transport the boulders under free-rolling transport modes were 6.07 and 6.12 m/s for 2° and 5° slopes respectively. For joint-bounded boulders, the minimum velocities are 9.39 and 9.53 m/s for 2° and 5° slopes respectively. These velocities are higher than the maximum velocities experienced at this particular locality during the great 26 December 2004 Indian Ocean tsunami, the largest known tsunami in recorded history. Because this tsunami flooded the area but did not result in appreciable damage to infrastructure, it is concluded that the imbricated boulders on Batu Feringgi beach are the result of tropical storm activity in the past, rather than from recent or past tsunamis. The N coast of Penang is thus regarded as safe from the hazard of damaging tsunamis resulting from mega-earthquakes in the Sumatra-Andaman subduction zone, but the area is prone to tropical storm damage (with a return frequency of about 1 in 400 years), with wave velocities exceeding 6–9.5 m/s.

S. Master (✉)

Economic Geology Research Institute, School of Geosciences, University of the Witwatersrand, P. Bag 3, WITS 2050, Johannesburg, South Africa
e-mail: sharad.master@wits.ac.za

Keywords Imbricated boulders • Penang island • Malaysia • Hydrodynamic calculations

12.1 Introduction

Penang Island (Figs. 12.1 and 12.2) is one of the fastest developing regions of Malaysia, with growth especially in tourism and hi-tech manufacturing sectors (Lateh et al. 2011). With increasing development and concomitant population growth has come the increased risk of natural hazards, resulting in a renewed focus on the recognition and mitigation of such hazards on Penang. For example, there have been recent studies on the effects of seismicity on built structures (Fadzli 2007), on tsunami hazard on the west (Colbourne 2005) and north (Jahromi 2009) coasts, and on landslide hazards in Penang (Ahmad et al. 2006; Lee and Pradhan 2006; Pradhan and Saro 2010; Lateh et al. 2011). The Batu Feringgi area on the NW coast of Penang has one of the highest concentrations of tourist beach hotels and related infrastructure on the island, and is thus critical to the tourist economy of Penang and Malaysia.

Batu Feringgi beach was affected, like most of the coastline of the entire region, by the Great Indian Ocean tsunami generated by the great Sumatra-Andaman earthquake of 26th December 2004 (Lay et al. 2005, Fig. 12.3; Roy and Ismail 2006;

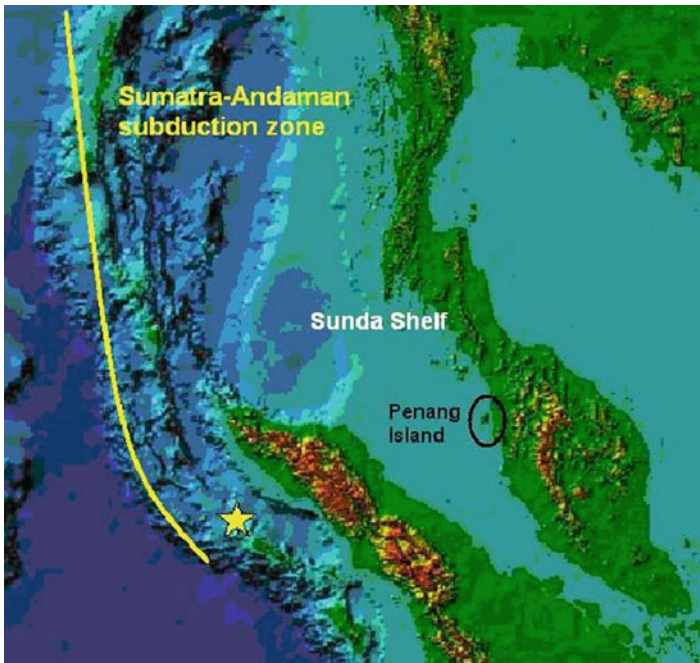


Fig. 12.1 The location of Penang Island, Malaysia (*enclosed in oval*), in relation to the stable Sunda Shelf, and the tectonically active Sumatra-Andaman subduction zone. The *yellow star* represents the epicentre of the great 26 December 2004 Sumatran earthquake, which then propagated northwards for 900 km along the Sumatra-Andaman fault (Lay et al. 2005; Neetu et al. 2005), and generated the great Indian Ocean tsunami of 26 December 2004



Fig. 12.2 Google Earth satellite view of Penang Island, with Batu Feringgi located at its northernmost end

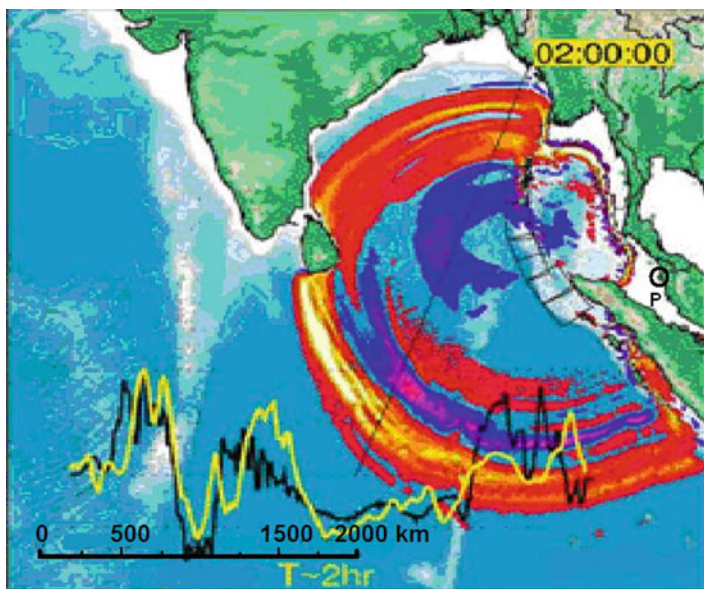


Fig. 12.3 Tsunami propagation model at time of 2.0 h after the great Sumatra-Andaman earthquake of 26 December 2004 (From Lay et al. 2005). The red colours are peaks and blue colours are troughs in the tsunami waves. Note the location of Penang Island (circle with P), in the Sunda Shelf, where much smaller tsunami waves were experienced, compared to the Bay of Bengal and the open Indian Ocean

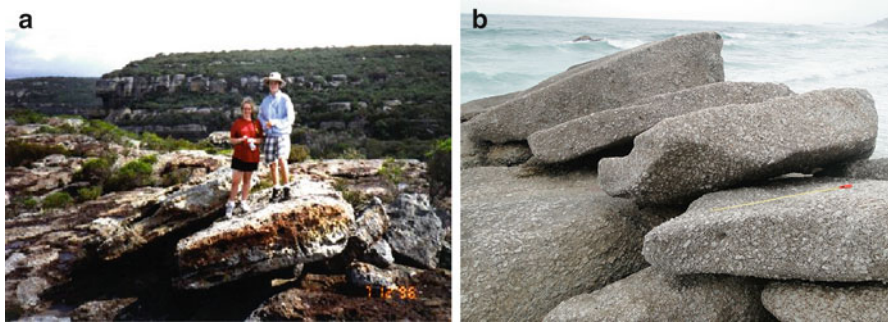


Fig. 12.4 (a) Imbricated rock slabs, thought to have been produced by ancient tsunamis. (a) Imbricated slabs, situated 32 m above sea level, at Mermaids Inlet, Jervis Bay, New South Wales, Australia. Photo courtesy of Ted Bryant, University of Woollongong. (b) Imbricated granite slabs, Clifton Beach, Cape Town, South Africa (After Master 2011). Measuring tape is 1 m long

Roy et al. 2007). However, unlike areas further north in Thailand, which were severely affected by the tsunami (Goto et al. 2010a), the Batu Feringgi area suffered little infrastructural damage, even though the area was inundated by large waves up to 3.3 m high (Roy and Ismail 2006; Roy et al. 2007) which flooded beach hotel grounds, and about a dozen or more people were reported as having been killed. The author discovered large imbricated granite boulders on the NE end of the tourist beach in the Batu Feringgi area. Since seaward-dipping imbricated boulders have been used as evidence for tsunami activity in other areas (Bryant et al. 1992; Young et al. 1996; Master 2011) (Fig. 12.4), it was decided to investigate the Batu Feringgi imbricated boulders further, and to study their relevance to tsunami hazards in NW Penang. In particular, it was important to know if such imbricate boulders were the result of the 26th December 2004 tsunami, or earlier tsunamis, or some other process, such as storm activity, which has recently been proposed as a source of much boulder movement along coastlines (Williams and Hall 2004; Switzer and Burston 2010; Etienne and Paris 2010; Cox et al. 2012), since both tsunamis and storms can deposit imbricated boulders.

12.2 Geological Setting

Penang Island is situated off the west coast of Peninsular Malaysia, and is composed of rocks similar to those which constitute the mainland (Kwan et al. 1992; Ong 1993). The rocks of the Malay peninsula have been divided into three tectonic domains, the granitic West Coast and East Coast provinces (Bignell and Snelling 1977), separated by the thin medial Central Province. These are now called the

Western, Central and Eastern Belts of Malaysia (Tate et al. 2008). The Western and Central Belts are separated by the Bentong-Raub suture zone, representing a collision zone between the two provinces (Hutchison 1977). The Western Belt is part of the North-Thailand-West Malaya Main Range province, which has mainly S-type biotite granites and abundant tin mineralization of Mid to Late Triassic age (Bignell and Snelling 1977; Liew and McCulloch 1985; Azman 2000; Searle et al. 2012). The Central and Eastern Belts (or East Malaya province) consist predominantly of Permian-Triassic I-type hornblende-biotite granites (Searle et al. 2012).

Three episodes of granite emplacement at 307 ± 8 Ma, 251 ± 7 Ma and 211 ± 2 Ma have been suggested for Penang and the NW Main Range province, based on Rb-Sr dating (Bignell and Snelling 1977; Kwan et al. 1992). However, all the granites have been affected by a hydrothermal conductive convection system related to the late Triassic intrusions (Kwan et al. 1992). Recent U-Pb zircon dating of granites from near Kuala Lumpur has yielded ages of 215 ± 7 to 210 ± 7 Ma (Searle et al. 2012).

Penang Island is underlain by two main granite plutons, the North Penang Pluton, composed of biotite-orthoclase granite, and the South Penang Pluton, composed of biotite-muscovite-microcline granite (Ong 1993). The North Penang Pluton has been divided into three major units known as the Tanjung Bungah granite, the Feringgi granite, and the Muka Head microgranite (Ong 1993). The granites on Penang have been dated at 215 ± 6 Ma and 209 ± 2 Ma (Liew and McCulloch 1985). The biotite and muscovite granites of Penang Island have been extensively weathered (Geological Survey of Malaysia 1992; Ahmad et al. 2006). Fission track work on Penang granites has shown that the island suffered a major episode of tilting and uplift in the Oligocene/Miocene (Kwan et al. 1992), since when there has been uplift and erosion of a formerly buried granite body. The western and southern parts of the island have a thin veneer of late Cenozoic sedimentary cover, and there are thick soils of Pleistocene to Holocene age (Geological Survey of Malaysia 1992; Ahmad et al. 2006). At the present day, the Malaysian Peninsula and Penang Island are part of the stable and aseismic Sunda Shelf. The closest tsunamigenic fault zone is the Sumatran-Andaman subduction zone reverse fault along the plate boundary between the Indo-Australian Plate and the SE Asian Plate. The island has rugged topography in its interior, with a highest elevation of 735 m, and a narrow coastal zone where the beaches are, with the elevation rising rapidly to over 100 m within a few hundred metres from the coastline. The beaches on Penang are situated in those few places where the elevation is less than 15 m (Fig. 12.5).

The Batu Feringgi area of Penang Island is underlain by the Feringgi biotite granite (Ong 1993). Petrographically, this granite is composed of quartz, orthoclase, microcline, plagioclase, biotite, and minor muscovite (Ahmad et al. 2006). Some varieties are porphyritic, with large alkali feldspar phenocrysts; other varieties contain large pockets of tourmaline.

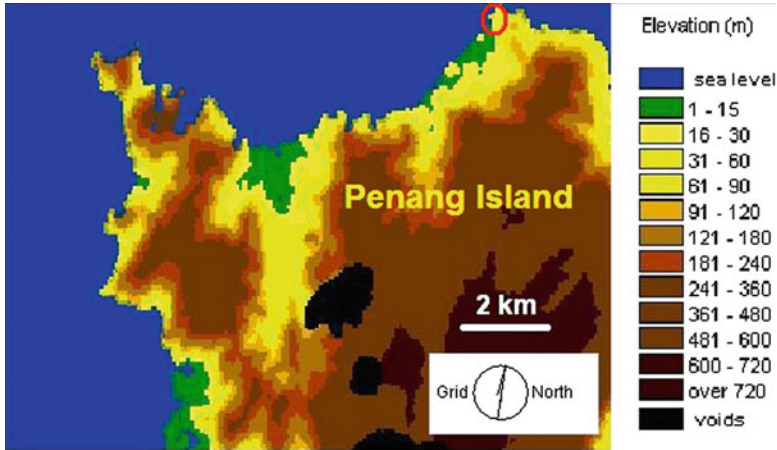


Fig. 12.5 Digital elevation model for NW Penang Island, after Anon (2011), modelled from ASTER satellite data obtained from GDS (2011). The beaches are found in areas with average elevation less than 15 m (shown *green*), along the west and north coasts. The locality of the imbricated boulders on Batu Feringgi beach is in the extreme north of the island, indicated with a *red oval*

12.3 Imbricate Boulders on Batu Feringgi Beach

The locality of the imbricate boulders is at $5^{\circ}28'51.77''\text{N}$, $100^{\circ}15'72''\text{E}$, in the Batu Feringgi district, northwest Penang, at the northeast end of the long sandy beach of Batu Feringgi, at the start of the rocky headland (having an elevation of up to 30 m) that forms the northernmost point of Penang Island (Figs. 12.5 and 12.6). Here loose granite boulders are arranged landward of a granitic outcrop which contains steep northward-dipping joints (Fig. 12.7).

There are three boulders (labeled 1, 2 and 3, Fig. 12.8) which are arranged in an imbricate fashion, with steep northward (seaward) dips of 45° , 65° and 70° respectively. The boulders are tabular in shape, and are roughly rectangular or in the shape of parallelepipeds with rounded corners. Although their exact shapes and hence masses are not known, a rectangular box derived from their axial dimensions a , b and c (with $a > b > c$) would indicate the maximum masses of the boulders, which are calculated as 2.3, 1.1 and 2.4 tonnes for boulders 1, 2 and 3 respectively (Fig. 12.8, Table 12.1). The shapes of the boulders were dictated by the presence of joints in the coastal outcrops, which represent an uplifted and exhumed tropically-weathered granite-tor landscape with residual soils (Ahmad et al. 2006). Boulders that have moved recently can be recognized from the occurrence of striae, crush zones, fresh scars or percussive marks (Etienne and Paris 2010). Such features generally occur when boulders move over a rock platform or limestone terrace, which is absent at Batu Feringgi beach. No such features were found on the imbricated boulders in the present study, indicating that they were probably not of recent origin, but had been subjected to marine erosion for long enough to have



Fig. 12.6 Google Earth satellite view of northern Penang Island, showing Batu Feringgi Beach and the locality of the imbricated granite boulders discussed in this study



Fig. 12.7 Loose boulders (numbered) at the northeast end of Batu Feringgi Beach, which are banked up against a rocky jointed granite headland. Note sitting person (on *left* hand side) for scale



Fig. 12.8 Imbricate arrangement of three boulders (1, 2 and 3), which are analysed in this study. The large granite mass behind boulder 1 is an outcrop, rather than a loose boulder

Table 12.1 Physical parameters for imbricated boulders

Boulder	a (m)	b (m)	c (m)	c/b	c^2/b^2	Density (g/cm^3)	Max. mass (tons)
1	1.50	1.32	0.44	0.33	0.11	2.71	1.2
2	1.25	0.75	0.44	0.59	0.34	2.71	1.1
3	2.20	0.85	0.47	0.55	0.31	2.71	1.3

obliterated any trace of such damage resulting from transport. The absence of adhering barnacles, limpets or seaweed attachment scars rules out the recent transport of the boulders from the intertidal zone, and they may have been moved only a few metres.

12.4 Hydrodynamic Calculations

Boulders transported by moving water can be moved by three different locomotion modes- sliding, rolling, and saltation, and different hydrodynamic factors are involved in each mode. The hydrodynamic equations for the initiation of boulder transport were originally obtained by Nott (1997, 2003), and are called the Nott equations. These equations have been used widely to model boulder transport by storms and tsunamis (Mastronuzzi and Sansò 2000; Kennedy et al. 2007; Scicchitano et al. 2007; Imamura et al. 2008; Etienne and Paris 2010; Switzer and Burston 2010; Goto et al. 2010b; Costa et al. 2011). Nandasena et al. (2011)

modified the Nott equations, based partly on the work of Voropayev et al. (2003) and Nanayama and Shigeno (2006), and produced a new set of hydrodynamic equations governing boulder transport initiation.

The conditions for the initiation of transport of a submerged or subaerial boulder under sliding mode are given by the modified Nott equation (Nandasena et al. 2011), as follows:

$$u^2 \geq 2([\rho_s/\rho_w] - 1)gc(\mu_s \cos \theta + \sin \theta)/[C_d(c/b) + \mu_s C_l] \quad (12.1)$$

where

u = fluid velocity required to initiate boulder movement	ρ_s = density of boulder
ρ_w = density of fluid	g = acceleration due to gravity
c = length of shortest axis of boulder	θ = angle of slope
b = length of intermediate axis of boulder	C_d = coefficient of drag
μ_s = coefficient of static friction	C_l = coefficient of lift

In order to produce imbrication of several boulders, the mode of transport has to be rolling/overturning. Initiation of boulder transport under rolling mode requires higher water velocities than the initiation of boulder movement under sliding conditions. For the case of rolling or overturning boulder movement initiation, the modified Nott equation (Nandasena et al. 2011) is as follows:

$$u^2 \geq 2([\rho_s/\rho_w] - 1)gc(\cos \theta + [c/b]\sin \theta)/[C_d(c^2/b^2) + C_l] \quad (12.2)$$

According to Nandasena et al. (2011), initial transport of a submerged or subaerial boulder will be in saltation mode when:

$$u^2 \geq 2([\rho_s/\rho_w] - 1)gc \cos \theta/C_l \quad (12.3)$$

For joint-bounded boulders, movement is initiated when

$$u^2 \geq 2([\rho_s/\rho_w] - 1)gc(\cos \theta + \mu_s \sin \theta)/C_l \quad (12.4)$$

Following Noormets et al. (2004) and Nandasena et al. (2011), the fluid density is that of seawater, taken as 1.02 g/cm³; the acceleration due to gravity is 9.81 m/s²; and the coefficients of drag (C_d), static friction (μ_s) and lift (C_l) are taken as 1.95, 0.7 and 0.178, respectively. The mean density of the Batu Feringgi granite is 2.71 g/cm³ (Ahmad et al. 2006). The slope on the Teluk Bahang beach is very flat, and is taken as 2°. Because the offshore topography is unknown, additional calculations were made for a slope of 5°. The physical parameters for the imbricated boulders are given in Table 12.1, and the results of the calculations are given in Table 12.2.

Table 12.2 Calculated flow velocities of seawater needed to initiate boulder movement (u_{\min}) under different transport modes (sliding, rolling/overturning and saltating), for loose boulders in submerged and subaerial settings only, at slopes of $\theta = 2^\circ$ and $\theta = 5^\circ$

Bldr	Sliding mode		Rolling mode		Saltating mode		Joint-bounded	
	u_{\min}	u_{\min}	u_{\min}	u_{\min}	u_{\min}	u_{\min}	u_{\min}	
	(m/s)	(m/s)	(m/s)	(m/s)	(m/s)	(m/s)	(m/s)	
	$\theta = 2^\circ$	$\theta = 5^\circ$	$\theta = 2^\circ$	$\theta = 5^\circ$	$\theta = 2^\circ$	$\theta = 5^\circ$	$\theta = 2^\circ$	$\theta = 5^\circ$
1	3.72	3.83	6.07	6.12	8.97	8.96	9.08	9.23
2	2.88	2.97	4.17	4.23	8.97	8.96	9.08	9.23
3	3.07	3.17	4.46	4.52	9.27	9.26	9.39	9.53

12.5 Discussion

Because the boulders are imbricated, their transport mode must have been rolling/overturning. The imbrication is produced by bedload transport, and boulder to boulder interaction, and the imbricated boulders dip upstream (in this case, offshore), in the direction from which the currents were coming. For each slope angle ($\theta = 2^\circ$ and $\theta = 5^\circ$), the highest velocity needed to initiate movement of any of the three boulders is taken as the minimum velocity of flow that would have moved all three boulders together (in order to produce the imbricate stacking observed). Since the imbricated boulders are stacked among jointed outcrops of granites, calculations were also made for the minimum velocities required to initiate boulder movement in joint-bounded mode, in addition to the calculations made for the case of free-standing boulders (Table 12.2).

The calculated minimum velocities required to initiate rolling/overturning of the imbricated boulders range from 6.07 ($\theta = 2^\circ$) to 6.12 ($\theta = 5^\circ$) m/s for rolling mode, to 9.39 ($\theta = 2^\circ$) and 9.53 ($\theta = 5^\circ$) m/s for joint-bounded mode. It could be argued that the particular values of the coefficients of lift (C_l), and static friction (μ_s) used in the equations of Nandasena et al. (2011) may not be valid for this case. So a sensitivity analysis was made, in which the coefficients of static friction (μ_s) and of lift (C_l) were varied by a factor of two (separate calculations were done using half and twice the values used by Nandasena et al. 2011, which originate from Noormets et al. 2004). As an example of these calculations, the u_{\min} value for boulder 1 at $\theta = 5^\circ$, under joint-bounded conditions, which was calculated as 9.23 m/s using the μ_s value of 0.7 from Noormets et al. (2004) (Table 12.2), yielded u_{\min} values of 9.08 and 9.48 for μ_s values of 0.35 and 1.4 respectively. So varying the coefficient of static friction (μ_s) by a factor of two results only in a $\pm 3\%$ change in the values of minimum velocities required to initiate boulder movement. The effect of changing the coefficient of lift (C_l) is much larger, yielding u_{\min} values of 6.52 m/s for a C_l values of 0.356, and 16.04 m/s for a C_l value of 0.059, compared to the Noormets et al. (2004) value of 0.178 used in Table 12.2. If the density of seawater is changed from the 1.02 g/cm³ used in the calculations (Table 12.2) to a value of 1.5 g/cm³, to allow for a turbulently mixed muddy ocean, then the u_{\min} value for boulder 1 falls from 9.23 to 6.48 m/s. The sensitivity analysis shows that

even if many of the coefficients used in the calculations presented in Table 12.2 were varied by a factor of 2, the results would still yield minimum velocities in the range 6–9.5 m/s in order to initiate the movement of the imbricated boulders under free standing and joint-bounded conditions. These velocities are higher than the maximum velocities experienced at this specific locality during the great 26 December 2004 Indian Ocean tsunami, the largest known tsunami in recorded history.

A number of video recordings of the incoming tsunami waves on 26th December 2004 were captured by tourists on the north coast of Penang Island, and are available for viewing on YouTube (Videos 12.1, 12.2, and 12.3). Analysis of Video 12.1, taken at Tanjung Bungah some 3 km east of Batu Feringgi, and which includes footage of tsunami waves passing by the mosque called Masjid Terapung, which is built on the coast on a promontory at right angles to the main trend of the coastline, has allowed for relatively accurate measurement of wave velocities. The wave passes by the Masjid Terapung, which has dimensions of 77 m (obtained from Google Earth), in 15 s, which gives an open-water incoming wave velocity (before run-up), of about 5.1 m/s. The video also shows that as the waves reached the shoreline, the velocities decreased rapidly in shallow water (although the actual velocities could not be quantified from the video because of a lack of measurable landmarks). The measured wave heights recorded at Tanjung Bungah were 3.0 m (Roy and Ismail 2006; Roy et al. 2007). Since the velocity of tsunami waves is equal to the square root of the depth multiplied by the acceleration due to gravity (9.81 m/s^2), it means that as the waves approach the shore (i.e., during run-up) their velocities decrease exponentially, and their amplitudes increase (e.g., Okal 1988). Another video (Video 12.2), taken on Batu Feringgi beach, shows a narrow shoreline of about 10 m, which was traversed by the first incoming tsunami wave in 3 s, giving a wave velocity of about 3.3 m/s. The water brought in by the first wave was about 0.5 m deep, which would have been just sufficient to cover the imbricated boulders. A third video, taken from a hotel window, shows tsunami waves coming in parallel to a sea-wall, and moving at a rate of about one car-length per second, or about 3 m/s. Videos 12.2 and 12.3 do not record the largest waves to have hit Batu Feringgi, since the highest measured wave heights there were recorded as 3.3 m above mean sea level (Roy and Ismail 2006; Roy et al. 2007).

The run-up wave heights and wavelengths of tsunami waves hitting a shoreline are strongly dependent on local conditions. The best studied tsunami is the 11 March 2011 Japanese Tohoku tsunami, for which the instrumentally-recorded data set contains the most comprehensive collection of coastal and deep-ocean observations ever made during a single tsunami event. From this event, more than 350 coastal water level records show regions of signal attenuation and amplification due to refraction, reflection, and bathymetric focusing (Eble et al. 2012).

Similarly, during storm events, wave behavior is strongly influenced by local conditions. According to Regnaud et al. (2004), bathymetric complexities exercise significant controls on wave refraction patterns during storms, and have resulted in significant variability in coastal response during storms in western France. Another factor of great importance is the storm surge, resulting from the pile up

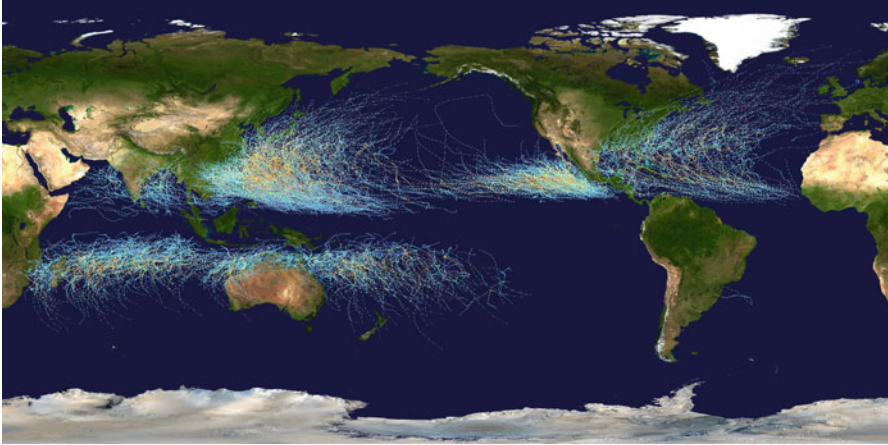


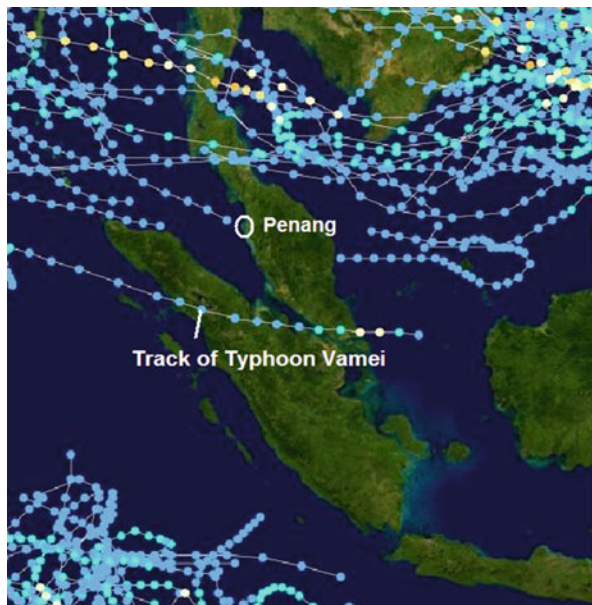
Fig. 12.9 Map of global tropical cyclone tracks recorded from 1985 to 2005. Compiled by Nilfanion (2006), with background image from NASA

of wind-driven waters from the continental shelves onto the coastal areas (Coch 1994; Flather 2003). Bathymetric factors such as water depth and slope are thus expected to control the velocities, wavelengths and propagation directions of waves on Batu Feringgi beach during storms, as well as during tsunami events.

Penang Island is less than 5.5° from the Equator, and hence is generally thought to be relatively free from the effects of major tropical storms or hurricanes, which, for reasons to do with global atmospheric vorticity, are mainly confined in subequatorial belts between 10° and 30° north and south of the Equator (McBride 1995) (Fig. 12.9). However, on 26th December 2001, typhoon Vamei was formed at 1.4°N in the southern South China Sea in what was previously deemed a cyclone-free equatorial zone, strengthened quickly, and made landfall along the southeast coast of Malaysia 60 km northeast of Singapore, and dissipated over Sumatra on 28th December 2001 (Fig. 12.10). The wind speeds were calculated to be as high as 36 m/s in the southern South China Sea, and would have generated wind waves with wave heights as high as 7.5 m on the southeast coast of Malaysia (Mohammed et al. 2012). An analysis by Chang et al. (2003) suggested that the return frequency for such a typhoon is approximately 1 in 400 years, which could also be taken as the return frequency for similar typhoons or tropical storms affecting Penang Island.

The question of whether boulders are moved by tsunami waves or storm waves is still a hotly debated issue, because the processes are quite similar, and it is difficult to unequivocally prove one mechanism of formation to the exclusion of the other (Williams and Hall 2004; Switzer and Burston 2010; Etienne and Paris 2010; Cox et al. 2012; Lau et al. 2012; Seshachalam et al. 2012). The Batu Feringgi beach appears to be fortuitously situated far enough from the seismogenic and tsunamigenic Sumatra-Andaman fault zone to be on the fringe of the area most prone to devastating effects of megatsunamis generated by the largest earthquakes generated in that region. Yet it contains boulders that were moved by waves with a

Fig. 12.10 Close-up view of SE Asia region in global map of tropical cyclone tracks from 1985 to 2005 (From Nilfanion 2006). The track in the centre of the image is from typhoon Vamei, 26–28 December 2001 (Chang et al. 2003)



minimum calculated velocity which was much higher than experienced in that particular location during the largest tsunami event ever recorded. It is possible that some previous pre-historic tsunami could have moved these boulders, but the chances are rather small, since the return frequency for tsunamigenic mega earthquakes, similar to or larger than the magnitude 9.2 earthquake of 26 December 2004 along the Sumatra-Andaman subduction zone, is of the order of millennia (McCaffrey 2008). The imbricated boulders, located at sea level, would be unlikely to have escaped erosion by attrition in this high-energy marine environment over such a length of time. The tectonic situation of Penang Island in the stable Sunda Straits also means that it is not prone to tsunamis generated by landslides on the continental shelf, most of which are triggered by seismic activity (Ward 2001; Nadim et al. 2005). In this case, tsunamis can effectively be ruled out as the causative agents, and it leaves the agency of rare (but not unknown) tropical storms, such as Vamei of 2001, as the most likely cause of the boulder movements on Batu Feringgi.

12.6 Conclusions

The Malaysian Peninsula and Penang Island are part of the stable and aseismic Sunda Shelf. The closest tsunamigenic fault zone is the Sumatran-Andaman subduction-zone reverse fault along the plate boundary between the Indo-Australian Plate and the SE Asian Plate. The 26 December 2004 Sumatra-Andaman

earthquake produced a tsunami that flooded the Batu Feringgi area of north Penang Island, but did not result in appreciable damage to infrastructure. The measured wave run-ups were up to 3.3 m above mean sea-level on Batu Feringgi, and the incoming wave velocities were in the range of 3–5 m/s, based on video analysis. However, the minimum velocities required to initiate movement of the imbricate boulders from Batu Feringgi were calculated to be in the range of 6–9.5 m/s. Hence it is concluded that the imbricated boulders on Batu Feringgi beach are the result of tropical storm activity in the past, rather than from the recent tsunami. If the magnitude 9.2 Sumatra-Andaman earthquake of 26 December 2004 (one of the strongest ever recorded) could not produce a sizeable tsunami on the north coast of Penang, then it is unlikely that any recent tsunami could have produced the imbricated boulders at Batu Feringgi, leaving tropical storms as the most likely culprit. The north coast of Penang (including Batu Feringgi beach) is thus regarded as safe from the hazard of damaging tsunamis resulting from mega-earthquakes in the Sumatra-Andaman subduction zone, but the area is prone to rare tropical storm damage, with wave velocities exceeding 6–9.5 m/s.

Acknowledgements I am grateful to Vicente Santiago-Fandiño and Yevgeniy Kontar for their comments. I also thank Grahame Oliver and An Yi Lau (National University of Singapore) and Ray Durrheim (CSIR/University of the Witwatersrand) for discussions. I am indebted to two anonymous reviewers who helped to improve the paper. Financial support from the South African National Research Foundation to attend the AOGS-AGU Joint Assembly in Singapore (August, 2012) is gratefully acknowledged.

References

- Ahmad F, Yahaya AS, Farooqi MA (2006) Characterization and geotechnical properties of Penang residual soils with emphasis on landslides. *Am J Environ Sci* 2(4):121–128
- Anon (2011) Penang- landforms. <http://www.geoscience-environment.com/es771/penang.htm>
- Azman AG (2000) The western belt granite of Peninsular Malaysia: some emergent problems on granite classification and its implication. *Geosci J* 4(4):283–293
- Bignell JD, Snelling NJ (1977) Geochronology of Malayan granites. *Overseas geology and mineral resources*, vol 47. IGS, London
- Bryant EA, Young RW, Price DM (1992) Evidence of tsunami sedimentation on the southeastern coast of Australia. *J Geol* 100:753–765
- Chang CP, Liu C-H, Kuo H-C (2003) Typhoon Vamei: an equatorial tropical cyclone formation. *Geophys Res Lett* 30:1150. doi:10.1029/2002GL016365, 4 pp
- Coch NK (1994) Geologic effects of hurricanes. *Geomorphology* 10:37–63
- Colbourne FW (2005). Tsunami impact on the West Coast of Penang Island, Malaysia. Research Project Report, M.S. in Physical Sciences, Emporia State University, Emporia, Kansas, USA
- Costa PJM, Andrade C, Freitas MC, Oliveira MA, da Silva CM, Omira R, Taborda R, Baptista MA, Dawson AG (2011) Boulder deposition during major tsunami events. *Earth Surf Proc Land* 36:2054–2068
- Cox R, Zentner DB, Kirchner BJ, Cook MS (2012) Boulder ridges on the Aran Islands (Ireland): recent movements caused by storm waves, not tsunamis. *J Geol* 120:249–272
- Eble M, Mungov G, Rabinovich A, Harris E, Titov V (2012) Spatial and temporal characterization of the 11 March 2011 tsunami. Abstracts, AOGS-AGU (WPGM) Joint Assembly, 13–17 Aug 2012, Singapore, Abstract No. OS07-17-A029 (CD-ROM)

- Etienne S, Paris R (2010) Boulder accumulations related to storms on the south coast of the Reykjanes Peninsula, Iceland. *Geomorphology* 114:55–70
- Fadzli MN (2007) Development of design response spectra for Penang Island. M.Sc. thesis (unpublished), Universiti Sains Malaysia, Penang, Malaysia
- Flather RA (2003) Storm surges. In: Holton JR et al (eds) *Encyclopedia of atmospheric sciences*. Academic, New York, pp 109–117
- GDS (2011) ASTER GDS Web Site, Earth Remote Sensing Data Analysis Center. http://gds.aster.ersdac.jspacesystems.or.jp/gds_www2002/index_e.html
- Geological Survey of Malaysia (1992) Quaternary geological map of Penang, Seberang Prai and Kuala Kurau
- Goto K, Okada K, Imamura F (2010a) Numerical analysis of boulder transport by the 2004 Indian Ocean tsunami at Pakarang Cape, Thailand. *Mar Geol* 268:97–105
- Goto K, Kawana T, Imamura F (2010b) Historical and geological evidence of boulders deposited by tsunamis, southern Ryukyu Islands, Japan. *Earth-Sci Rev* 102:77–99
- Hutchison CS (1977) Granite emplacement and tectonic subdivisions of Peninsular Malaysia. *Geol Soc Malaysia Bull* 9:187–207
- Imamura F, Goto K, Ohkubo S (2008) A numerical model for the transport of a boulder by tsunami. *J Geophys Res* 113, C01008. doi:10.1029/2007JC004170
- Jahromi BI (2009) Design of a tsunami barrier to the north of Penang Island. M. Eng. (Civil-Hydraulics and Hydrology) dissertation, Faculty of Civil Engineering, Universiti Teknologi Malaysia, 86 pp
- Kennedy DM, Tannock KL, Crozier MJ, Rieser U (2007) Boulders of MIS 5 age deposited by a tsunami on the coast of Otago, New Zealand. *Sediment Geol* 200:222–231
- Kwan TS, Krähenbühl R, Jäger E (1992) Rb-Sr, K-Ar and fission track ages for granites from Penang Island, West Malaysia: an interpretation model for Rb-Sr whole-rock and for actual and experimental mica data. *Contrib Mineral Petrol* 111(4):527–542
- Lateh H, Khan MMA, Jefriza (2011) Monitoring of shallow landslide in Tun Sardon 3.9 km, Pinang Island, Malaysia. *Int J Phys Sci* 6(12):2989–2999
- Lau AYA, Etienne S, Terry J, Lee YS, Switzer S (2012) Preliminary findings on recent and ancient large-wave signatures in coastal reef-platform boulder fields from Makemo Atoll, French Polynesia. Abstracts, AOGS-AGU (WPGM) Joint Assembly, 13–17 Aug 2012, Singapore, Abstract No. OS14-A001 (CD-ROM)
- Lay T, Kanamori H, Ammon CJ, Nettles M, Ward SN, Aster RC, Beck SL, Bilek SL, Brudzinski MR, Butler R, DeShon HR, Ekström G, Satake K, Sipkin S (2005) The Great Sumatra-Andaman earthquake of 26 December 2004. *Science* 308:1127–1133
- Lee S, Pradhan B (2006) Probabilistic landslide hazards and risk mapping on Penang Island, Malaysia. *J Earth Syst Sci* 115(6):661–672
- Liew TC, McCulloch MT (1985) Genesis of granitoid batholiths of Peninsular Malaysia and implications for models of crustal evolution: evidence from a Nd-Sr isotopic and U-Pb zircon study. *Geochim Cosmochim Acta* 49:587–600
- Master S (2011) Transported megaboulders and the recognition of palaeotsunamites at Clifton Beach and surrounding areas, Cape Town, South Africa. Abstract Book, GeoSynthesis 2011 Conference and Exhibition, Integrating the Earth Sciences, 30 August–1 September 2011, Cape Town, pp 188–189
- Mastronuzzi G, Sansò P (2000) Boulders transport by catastrophic waves along the Ionian coast of Apulia (Southern Italy). *Mar Geol* 170:93–103
- McBride JL (1995) Tropical cyclone formation. In: Elsberry RL (ed) *Global perspectives on tropical cyclones*, World Meteorological Organization, Geneva, Report No. TCP-38. <http://derecho.math.uwm.edu/classes/TropMet/GPTC/tcclimo.pdf>
- McCaffrey M (2008) Global frequency of magnitude 9 earthquakes. *Geology* 36(3):253–266
- Mohammed A, Tkalic P, Vinod Kumar K, Vethamony P (2012) Hindcasting of wind waves generated by typhoon Vamei. Abstracts, AOGS-AGU (WPGM) Joint Assembly, 13–17 Aug 2012, Singapore, Abstract No. OS011-16-A006 (CD-ROM)

- Nadim F, Kvalstad T, Guttormsen T (2005) Quantification of risks associated with seabed instability at Ormen Lange. *Mar Pet Geol* 22:311–318
- Nanayama F, Shigeno K (2006) Inflow and outflow facies from the 1993 tsunami in southwest Hokkaido. *Sed Geol* 187:139–158
- Nandasena NAK, Paris R, Tanaka N (2011) Reassessment of hydrodynamic equations: minimum flow velocities to initiate boulder transport by high energy events (storms, tsunamis). *Mar Geol* 281:70–84
- Neetu S, Suresh I, Shankar R, Shankar D, Shenoj SSC, Shetye SR, Sundar D, Nagarajan B (2005) Comment on “The Great Sumatra-Andaman earthquake of 26 December 2004”. *Science*, 310, 1431, doi:10.1126/science.1118950
- Nilfanion (2006) Global tropical cyclone tracks. http://en.wikipedia.org/wiki/File:Global_tropical_cyclone_tracks-edit2.jpg
- Noormets R, Crook KAW, Felton EA (2004) Sedimentology of rocky shorelines: 3. Hydrodynamics of megaclast emplacement and transport on a shore platform, Oahu, Hawaii. *Sedim Geol* 172:41–65
- Nott J (1997) Extremely high wave deposits inside the Great Barrier Reef, Australia: determining the cause- tsunami or tropical cyclone. *Mar Geol* 141:193–207
- Nott J (2003) Waves, coastal boulders, and the importance of the pre-transport setting. *Earth Planet Sci Lett* 210:269–276
- Okal EA (1988) Seismic parameters controlling far-field tsunami amplitudes: a review. *Nat Hazards* 1:67–96
- Ong WS (1993) The geology and engineering geology of Pulau Pinang. Geological survey of Malaysia, Map report 7
- Pradhan B, Saro L (2010) Delineation of landslide hazard areas on Penang Island, Malaysia, by using frequency ratio, logistic regression and artificial neural network models. *Env Earth Sci* 60(5):1037–1054
- Regnaud H, Pirazzoli PA, Morvan G, Ruz M (2004) Impacts of storms and evolution of the coastline in western France. *Mar Geol* 210:325–337
- Roy GD, Ismail AIM (2006) Numerical modelling of tsunami along the coastal belt of Penang using a polar coordinate shallow water model. *Far East J Appl Math* 23(3):241–261
- Roy GD, Karim MF, Ismail AIM (2007) A nonlinear polar coordinate shallow water model for tsunami computation along North Sumatra and Penang Island. *Cont Shelf Res* 27:245–257
- Scicchitano G, Monaco C, Torcorici L (2007) Large boulder deposits by tsunami waves along the Ionian coast of south-eastern Sicily (Italy). *Mar Geol* 238:75–91
- Searle MP, Whitehouse MJ, Robb LJ, Ghani AA, Hutchison CS, Sone M, Ng SW-P, Roselee MH, Chung S-L, Oliver GJH (2012) Tectonic evolution of the Sibumasu-Indochina terrane collision zone in Thailand and Malaysia: constraints from new U-Pb zircon chronology of SE Asian tin granitoids. *J Geol Soc, London* 169(4):489–500
- Seshachalam S, Karthikeyan A, Switzer A, Gouramanis C (2012) Sedimentological characteristics of tsunami and storm deposits: a modern analog from Southeast Indian coast. Abstracts, AOGS-AGU (WPGM) Joint Assembly, 13–17 Aug 2012, Singapore, Abstract No. OS14-A013 (CD-ROM)
- Switzer AD, Burston JM (2010) Competing mechanisms for boulder deposition on the southeast Australian coast. *Geomorphology* 114:42–54
- Tate RB, Tan DK, Ng TF (2008) Geological map of Peninsular Malaysia. In: Hutchison CS, Tan NK (eds) *Geology of Peninsular Malaysia*. Geological Society of Malaysia, Kuala Lumpur, 479 p
- Voropayev SI, Testik FY, Fernando HJS, Boyer DL (2003) Morphodynamics and cobbles behaviour in and near the surf zone. *Ocean Eng* 30:1741–1764
- Video 1. Tsunami 2004 at Tanjung Bungah Penang. http://www.youtube.com/watch?feature=player_detailpage&v=IkPw0WSgWqc
- Video 2. Raw tsunami video Penang Beach Malaysia 2004. Uploaded by PubDom on 14 February 2007. http://www.youtube.com/watch?feature=player_detailpage&v=wJIDvzdB-Zg

- Video 3. Penang Tsunami. Uploaded by Adda58 (Jeff Addinsall) on 27 May 2008, shot at 2 PM, 26 December 2004. http://www.youtube.com/watch?feature=player_detailpage&v=NCWd21ortdk
- Ward S (2001) Landslide tsunami. *J Geophys Res* 106(6):11201–11215
- Williams DM, Hall AM (2004) Cliff-top mega-clast deposits of Ireland, a record of extreme waves in the North Atlantic- storms or tsunamis? *Mar Geol* 206:101–117
- Young RW, Bryant EA, Price DM (1996) Catastrophic wave (tsunami?) transport of boulders in southern New South Wales, Australia. *Zeitschrift für Geomorphologie* 40(2):191–207